Journal of Electrochemical Science and Technology
Vol. 2, No. 3, 2011, 136-142
DOI:10.5229/JECST.2011.2.3.136

Journal of Electrochemical Science and Technology

Polarization Behavior of $Li_4Ti_5O_{12}$ Negative Electrode for Lithium-ion Batteries

Ji Heon Ryu†

Graduate School of Knowledge-based Technology and Energy, Korea Polytechnic University, 2121 Jeongwang-dong, Siheung-si, Gyeonggi-do 429-793, Korea

ABSTRACT :

$Li_4Ti_5O_{12}$ is prepared through a solid-state reaction between Li_2CO_3 and anatase TiO_2 for applications in lithium-ion batteries. The rate capability is measured and the electrode polarization is analyzed through the galvanostatic intermittent titration technique (GITT). The rate characteristics and electrode polarization are highly sensitive to the amount of carbon loading. Polarization of the $Li_4Ti_5O_{12}$ electrode continuously increases as the reaction proceeds in both the charge and discharge processes. This relation indicates that both electron conduction and lithium diffusion are significant factors in the polarization of the electrode. The transition metal (Cu, Ni, Fe) ion added during the synthesis of $Li_4Ti_5O_{12}$ for improving the electrical conductivity also greatly enhances the rate capability.

Keywords: Lithium-ion batteries, Electrical conductivity, Polarization. $Li_4Ti_5O_{12}$, Rate capability

Received July 5, 2011 : Accepted August 14, 2011

1. Introduction

$Li_4Ti_5O_{12}$ is a promising negative electrode material for high-power and quick-charging lithium-ion batteries because of its excellent cycle performance and structural stability during charge–discharge cycles, with a theoretical capacity of 175 mAh/g.[1,2] The spinel structure of $Li_4Ti_5O_{12}$ provides a three-dimensional network of channels for facile lithium diffusion and exhibits an extremely small volume change during the cycles.

As $Li_4Ti_5O_{12}$ shows a flat reaction potential of 1.55 V (*vs.* Li/Li^+), which is higher than the reduction potentials of common electrolyte solvents, it does not form a solid electrolyte interface. These properties can be of great merit for high-power and quick-charging applications. However, despite these benefits, $Li_4Ti_5O_{12}$ does not yet meet all the requirements for successful use in high power applications due to its poor electrical conductivity and slow lithium ion diffusion. To improve the rate performance of $Li_4Ti_5O_{12}$, several methods have been proposed, including new synthetic methods for nanostructured or nanosized materials, doping with other metal ions and incorporation of carbon with high electronic conductivity. The use of nanostructured or nanosized particles facilitates the shortening of the pathway for lithium diffusion and enlargement of the available active surface.[3-6] Addition of a transition metal to the $Li_4Ti_5O_{12}$ increases the electrical conductivity by the formation of a double spinel structure or metal oxide composite.[7-9] Di- or trivalent cation doping at the Li-site and pentavalent cation doping at the Ti-site have been reported to increase the electrical conductivity through Ti^{3+} formation.[10-17] Furthermore, carbon coating on the $Li_4Ti_5O_{12}$ surface is a very effective way to construct electron pathway.[18-20]

In this work, we have prepared $Li_4Ti_5O_{12}$ powder through solid state reaction and measured the rate performance and electrode polarization through galvanostatic charge-discharge and galvanostatic intermittent titration technique (GITT).[21] As the rate performance is strongly related to the electrode polarization by the limitation of ohmic loss, charge transfer and mass transfer, we

†Corresponding author. Tel.: +82-31-8041-0326
E-mail address: ryujh@kpu.ac.kr

attempted to investigate polarization behavior of the polarization of the $Li_4Ti_5O_{12}$ electrode and the voltage transient during current interruption.

2. Experimental

Commercial Li_2CO_3 and TiO_2 (anatase) powders were used as Li- and Ti-precursors for $Li_4Ti_5O_{12}$ synthesis. Each dried powder was ball-milled with alumina ball and ethanol as dispersant by planetary miller for 1 hr at 350 rpm. These precursors were heat treated at 800°C for 12 h in air at a heating and cooling rate of 5°C/min. For the addition of transition metal, $CuSO_4 \cdot 5H_2O$, Fe_3O_4, and NiO were used by 5 mol% compared to the amount of lithium.

For the electrochemical tests, the composite electrodes were prepared by coating the slurry of active material, polyvinylidene fluoride (PVdF) binder, and conductive carbon (Denka black) (80 : 10 : 10, 90 : 5 : 5, and 95 : 3 : 2 in weight ratio in *N*-methyl-2-pyrrolidone solvent) on a piece of Al foil (thickness = 20 μm). The electrode plates were roll-pressed to enhance the inter-particle contact and to ensure the adhesion to the current collector and then dried in vacuum oven at 120 °C for 12 h. The loading amount of active mass in the electrodes was ~4 mg/cm^2. The coin-type cells (CR2032) were assembled in a glove box with Li foil as the counter electrode, 1.3 M $LiPF_6$ in EC : EMC (3 : 7 in vol. ratio, where EC is ethylene carbonate and EMC is ethylmethyl carbonate) as the electrolyte, and a porous polyethylene film as the separator.

The galvanostatic charge-discharge measurements were performed in a potential range of 1.0~2.5 V (versus Li/Li^+) at different current conditions of 0.1 *C* (17.5 mA/g)-4.0 *C* (700 mA/g). Each cycle was performed by constant current cycle by the same current was applied both charge (lithiation) and discharge (delithiation). The cells were charged and discharged for three cycles at each current density at 25 °C with a WBCS-3000 battery cycler (Wonatech Co.).

The galvanostatic intermittent titration technique (GITT) was employed to monitor the evolution of electrode polarization during cycling, where a current pulse of 0.1 *C* (17.5 mA/g) was applied for 10 min to measure the closed-circuit voltage (CCV) and turned off for 10 min to obtain the quasi-open-circuit voltage (QOCV). The sequential current pulse was applied for both charging and discharging period in the range of 1.0-2.5 V (*vs.* Li/Li^+). Polarization value was calculated from the difference between the CCV and QOCV in each current interruption step.

3. Results and discussion

Fig. 1 shows the FE-SEM images of the $Li_4Ti_5O_{12}$ powder. The particles formed necks to connect with each other, and the particle size was typically on the order of submicrons (ca. 500 nm). Fig. 2 displays the galvanostatic charge and discharge curves at three initial cycles at a constant current rate of 17.5 mA/g (0.1 *C*-rate) for a voltage range of 1.0~2.5 V (*vs.* Li/Li^+). Plateaus at the voltage of approximately 1.5 V correspond to the electrochemical lithium insertion and extraction. Based on the voltage curves of the cell with 5 wt.% carbon loading (shown in Fig. 2(a)), the charging and discharging capacities at the first cycle were 161.3 and 151.0 mAh/g, respectively. The overpotential of the $Li_4Ti_5O_{12}$ electrode at the second cycle was lesser with that of the initial cycle. The decrease of overpotential is expected to be induced by the activation of the working electrode and the Li counter electrode during the first cycle. After the

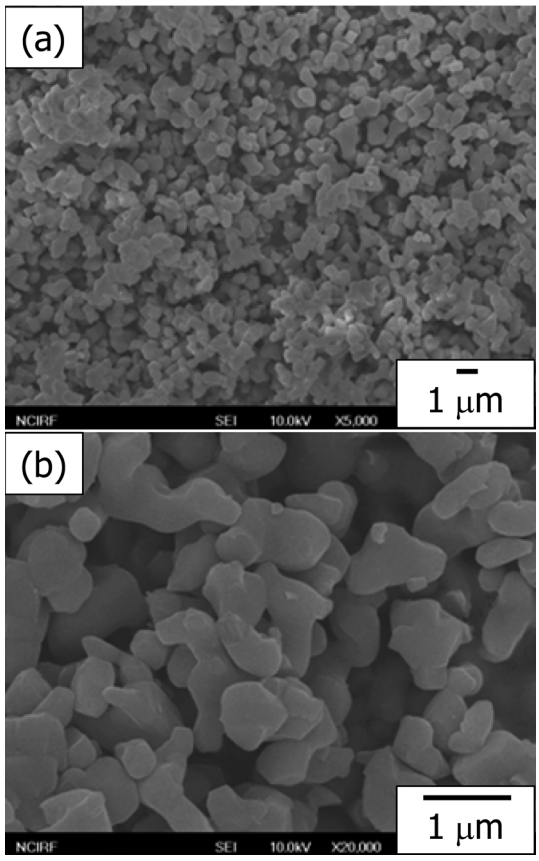

Fig. 1. FE-SEM images of the $Li_4Ti_5O_{12}$ prepared by solid state reaction at (a) 5000 times and (b) 20000 times.

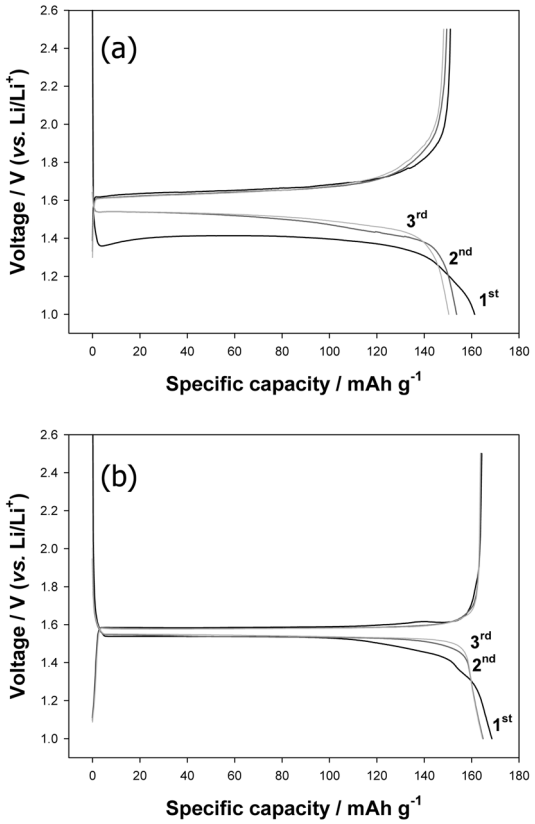

Fig. 2. The initial three charge-discharge voltage profiles obtained from the Li/$Li_4Ti_5O_{12}$ cell with (a) 5 wt.% and (b) 10 wt.% carbon loading. Charge/discharge rate = 0.1 *C* (17.5 mA/g). Voltage cut-off range = 1.0~2.5 V (*vs*. Li/Li^+).

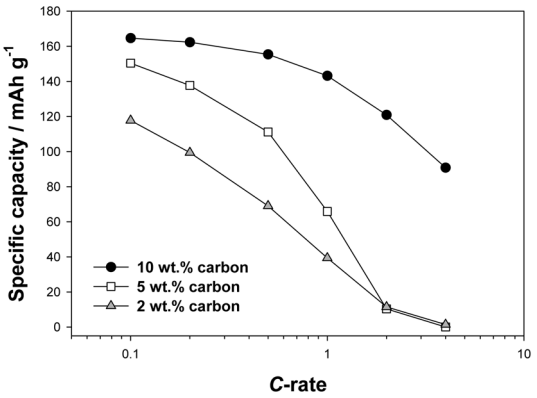

Fig. 3. Rate performances of the $Li_4Ti_5O_{12}$ cells at 0.1~4 *C* with variations in carbon loading. Voltage cut-off range = 1.0~2.5 V (*vs*. Li/Li^+).

first cycle, each voltage profile was almost the same as the second one. As the $Li_4Ti_5O_{12}$ electrode reacts with lithium via a two-phase reaction, the flat voltage plateau was expected to appear. However, it showed a sloping voltage curve similar to that of a one-phase reaction due to the large electrode polarization due to poor electron conduction. As seen in Fig. 2(b), the electrode with higher carbon loading, 10 wt.%, had flatter voltage profiles and higher specific capacities of 168.6 mAh/g during charging and 164.3 mAh/g during discharging of the electrode. This flatter profile and high specific capacity resulted from a smaller electrode polarization caused the efficient electron transfer pathway.

Fig. 3 shows rate characteristics of $Li_4Ti_5O_{12}$ with variation in carbon loading. The specific capacity and rate capability were found to improve with an increase in the carbon loading, which was consistent with previous results. As the amounts of carbon loading were increased, the capacity at 0.1 *C* (17.5 mA/g) was increased from 117.7 mAh/g. at 2 wt.% carbon to 164.6 mAh/g at 10 wt.% carbon. Moreover, the specific capacity rapidly decreased at high current conditions. In case of 10 wt.% carbon, a capacity of 90.8 mAh/g was achieved in spite of 4 *C* current (700 mA/g); this capacity amounts to 55% of capacity at the 0.1 *C* condition. Under 10 wt.% carbon loading, $Li_4Ti_5O_{12}$ hardly reacted with lithium at 4 *C* and its capacity was only about ~10 mAh/g at 2*C*. Through this result, we assumed that the electrochemical performance significantly depended on the electron conduction, which served as the polarization of the electrode.

The GITT was used to keep track of the polarization variation while the electrodes were being charged or discharged. Fig. 4 presents the overall transient voltage profile by the GITT of $Li_4Ti_5O_{12}$ electrode and Fig. 5 shows the behavior of electrode polarization with the state of charge (SOC) of 5 wt.% (a) and 10 wt.% (b) carbon loading in the third cycle. The quasi-open circuit voltage (QOCV) and closed-circuit voltage (CCV) can be obtained with these voltage profiles. When the current pulse is applied during charging, voltage increases to reach the CCV due to the ohmic loss, charge transfer and mass transfer resistance. As we turned off of current pulse, the voltage dropped to reach a QOCV as quasi-equilibrium value. The CCV profiles of both electrodes with different carbon loading showed very different characteristics, however, the QOCV profiles of two electrodes were very similar to each other. This profile suggests that the two electrodes undergo the same type

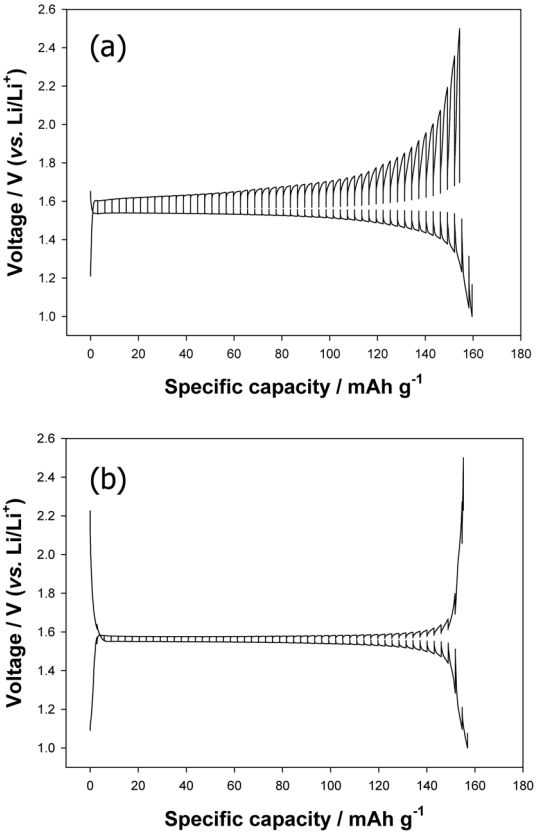

Fig. 4. Transient voltage profiles obtained with the $Li_4Ti_5O_{12}$ cells in the third cycle in (a) 5 wt.% and (b) 10 wt.% carbon.

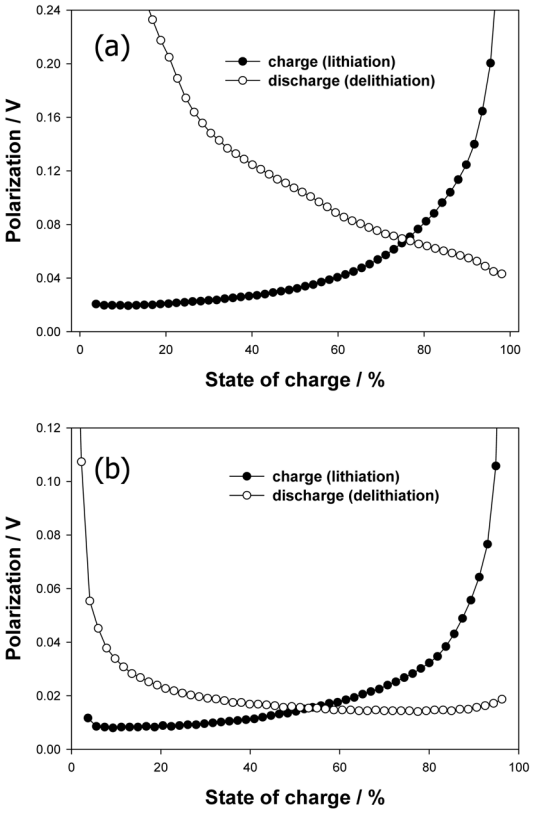

Fig. 5. State of charge (SOC) dependent polarization curves for the $Li_4Ti_5O_{12}$ electrode cells in the third cycle with (a) 5 wt.% and (b) 10 wt.% carbon.

of electrochemical reaction, but with a large gap in the polarization. Fig. 4(a) shows a flat voltage profile of QOCV and a larger sloping profile of CCV due to the continuous increasing of electrode polarization in 5 wt.% carbon loading.

The electrode polarization is defined as the difference between CCV and QOCV in each voltage transient. The electrode polarization with 5 wt.% carbon is twice that with 10 wt.% carbon during charging. The polarization behavior of both electrodes linearly increases at the beginning of the charging process (low SOC). As a charging reaction of $Li_4Ti_5O_{12}$ proceeds, $Li_4Ti_5O_{12}$ reacts with the lithium ion and the Ti^{4+} ions are reduced to the Ti^{3+}/T^{4+} mixed valence of higher electrical conductivity. The $Li_4Ti_5O_{12}$ powders therefore gradually became core/shell structures of $Li_4Ti_5O_{12}/Li_7Ti_5O_{12}$, as lithium could easily react with the surface of $Li_4Ti_5O_{12}$ powders.[22] Although electron conduction becomes faster, lithium has to penetrate the thicker $Li_7Ti_5O_{12}$ shell to the $Li_4Ti_5O_{12}$ core at the end of charging process (high SOC).

As the lithium insertion proceeded in the charging process, the increase of polarization started to rise rapidly over SOC60 with lower carbon loading. Similarly, polarization with higher carbon loading is also abruptly increased over SOC80. In this composite electrode with $Li_4Ti_5O_{12}$ and carbon black, the $Li_4Ti_5O_{12}$ powder and carbon particles are dispersed, resulting in a large contact area between the two components. When the carbon loading is higher, more $Li_4Ti_5O_{12}$ powders are directly connected to the electron conducting path of carbon black. After the directly connected $Li_4Ti_5O_{12}$ powders react with lithium, polarization of the electrode increases abruptly because the other powders, being isolated from the conduction path, have a large overpotential at the charging reaction due to the lacks of electron supply. For the complete reaction of these isolated powders, electrons and/or lithium ions have to move through the already reacted $Li_7Ti_5O_{12}$ particles.

As shown in Fig. 5, the polarization at the discharging

(delithiation) is larger than that at the charging (lithiation). As the lithium extracts from $Li_7Ti_5O_{12}$ particles, the surface of these particles are converted to the $Li_4Ti_5O_{12}$ phase which has a poor electrical conductivity.[22] Polarization with lower carbon loading continually increases during the discharging due to the insufficient path of electron and the formation of poor conduction phase at the surface.

Fig. 6 illustrates a voltage transient at both charging and discharging in variation with the SOC. The ohmic drop appeared due to the IR loss by electron conduction at the beginning of voltage transient; charge and mass transfer then occurred sequentially after current interruption. As shown in Fig. 6(a), ohmic loss of the electrode with lower carbon loading was almost constant until SOC50 and then abruptly increased; polarization by the charge transfer and mass transfer increased continuously. By the voltage transient of the electrode with higher carbon loading, polarization by ohmic loss was very small and almost constant until SOC70 because of effective electron conduction. Moreover, polarization by the charge transfer and mass transfer was also small because the larger number of electron pathways enlarged the reaction sites and shortened the average diffusion length. Fig. 6(b) and Fig. 6(d) show the voltage transient in the discharging.

The polarization in the discharging was larger than that of charging due to the surface formation of the $Li_4Ti_5O_{12}$ phase which has poor electrical conductivity. For the same reason, ohmic loss of the electrode with lower carbon loading was continuously increased during the discharging. Rapid increase of polarization by charge transfer and mass transfer was apparent. Poor electron conduction restricts the active sites where the charge transfer reaction takes place. In addition, the reduced reaction area lengthens the distance of lithium diffusion. As shown in Fig. 6(d), polarization of the electrode with higher carbon loading was maintained during the charging but increased at the end of discharge due to the limitations of charge transfer and mass transfer. Constant ohmic loss during discharging and a low overall polarization were able to be obtained by the supply with sufficient electron conductive path.

In order to improve the rate performance of the

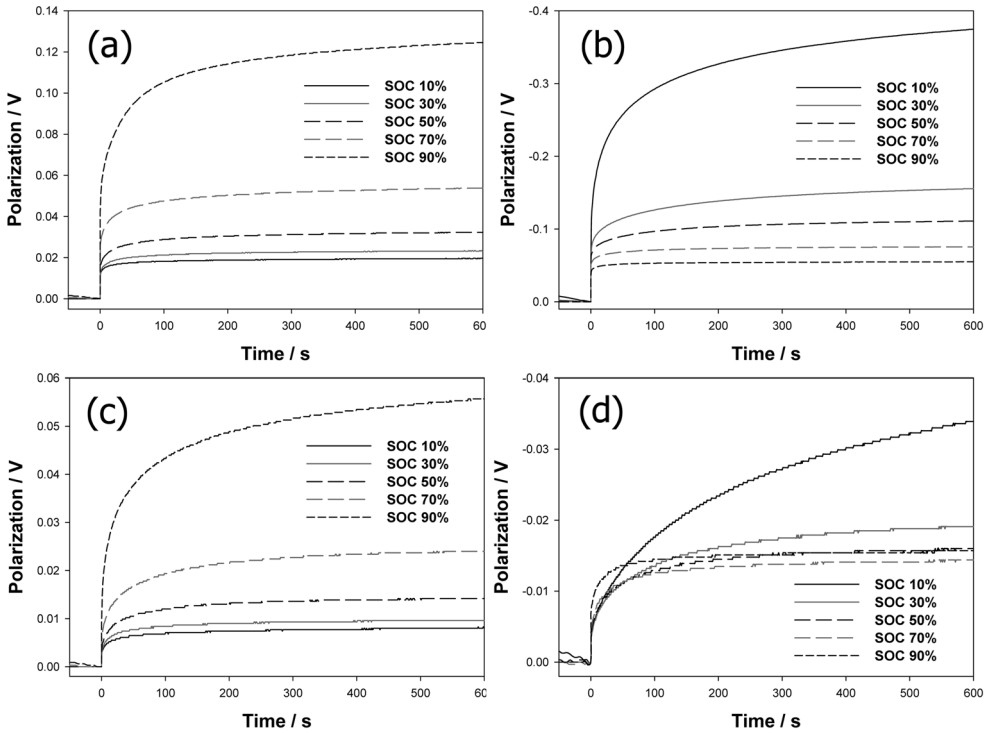

Fig. 6. Transient voltage profiles in a single current interruption step obtained with the $Li_4Ti_5O_{12}$ cells in the third cycle: (a) charging (lithiation) and (b) discharging (delithiation) steps in 5 wt.% carbon loading, (c) charging (lithiation) and (d) discharging (delithiation) steps in 10 wt.% carbon loading. Voltage profiles at the SOC10, SOC30, SOC50, SOC70, and SOC90 are given.

$Li_4Ti_5O_{12}$ electrode, it was essential to ensure the path of electron transfer. However, excessive use of carbon black presented two major problems. The first is the lowered energy density of the cell and the second is the complicated electrode fabrication process.

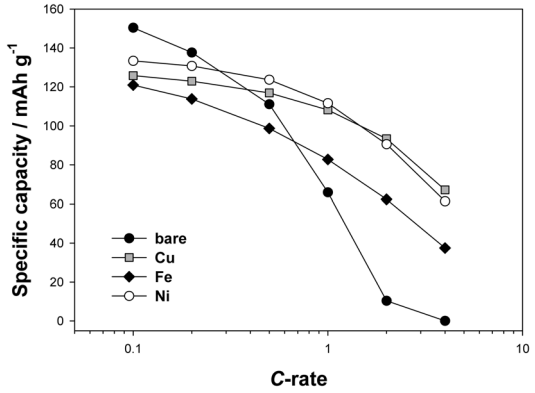

Fig. 7. Rate performances of the transition metal ion added $Li_4Ti_5O_{12}$ cells at 0.1~4 *C*. Voltage cut-off range = 1.0~2.5 V (*vs*. Li/Li^+).

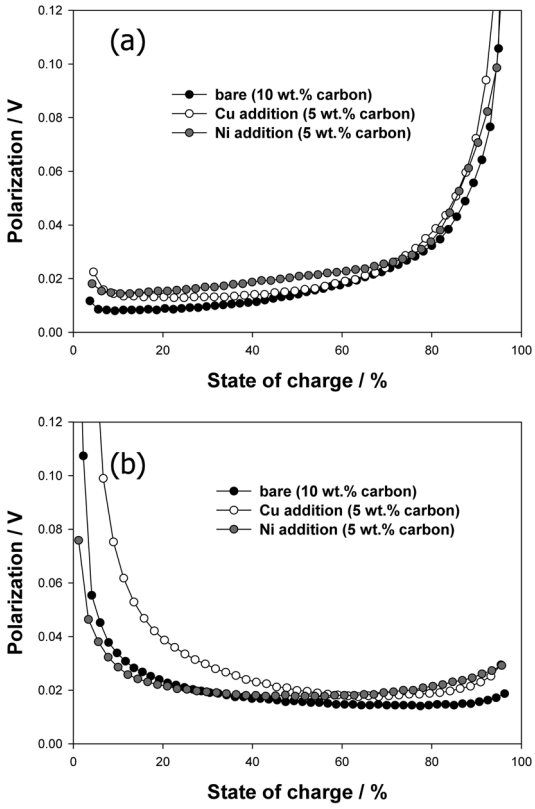

Fig. 8. State of charge (SOC) dependent polarization curves for the transition metal ion added $Li_4Ti_5O_{12}$ electrode cells in the third cycle at the (a) charging and (b) discharging.

By the 5 mol% addition of transition metal ions (Cu, Ni, Fe) which have higher electrical conductivity that of titanium oxide, the rate capability was enhanced. The rate performances are shown in Fig, 7. While the initial capacity decreased by 10~20% (121.0~133.4 mAh/g), significant improvement of the rate characteristics was achieved, especially in the case of Cu and Ni additions. The specific capacity in the case of Cu addition was 67.2 mAh/g at 4 *C* current, which amounts to 53% of the capacity at 0.1 *C* current, in spite of only 5 wt.% carbon black loading. The rate performance is approximately that of the value in 10 wt.% carbon loading (55% of the capacity at 0.1 *C* current).

In spite of only 5 wt.% carbon loading, the polarization of the Cu and Ni added $Li_4Ti_5O_{12}$ electrode is similar to that of the bare $Li_4Ti_5O_{12}$ electrode with 10 wt.% carbon loading. The addition of the transition for improving the electrical conductivity decreases the electrode polarization and also greatly enhances the rate performance.

Therefore, the efficient electron transfer path must be constructed, and the nanosized powders must be synthesized in order to improve the rate capability of $Li_4Ti_5O_{12}$. For the electrical conduction, the amount of carbon black or the electrical conductivity of active material should be increased.

4. Conclusion

$Li_4Ti_5O_{12}$ powder was synthesized by the solid-state reaction between Li_2CO_3 and TiO_2 for Li-ion battery applications. The following conclusions were made:

The rate characteristics and the polarization of the $Li_4Ti_5O_{12}$ electrode significantly depend on the amount of carbon loading for the electron conductive path.

The $Li_4Ti_5O_{12}$ electrode has a sloping voltage profile due to electrode polarization despite the two-phase reaction, especially in the case of lower carbon loading (5 wt.%). Polarization increases continuously as the reaction proceeds during the charge and discharge process due to the lithium diffusion in the $Li_4Ti_5O_{12}$ particle.

Rate performance was greatly improved by the addition of transition metal (Cu, Ni, Fe) ion for the increase of electrical conduction.

Acknowledgement

This work was supported by the Industrial Core

Technology Development Program funded by the Ministry of Knowledge Economy, Republic of Korea (Project No. 10035302).

References

1. K. M. Colbow, J. R. Dahn and R. R. Haering, *J. Power Sources*, **26**, 397 (1989).
2. K. Zaghib, M. Armand and M. Gauthier, *J. Electrochem. Soc.*, **145**, 3135 (1998).
3. J. Lim, E. Choi, V. Mathew, D. Kim, D. Ahn, J. Gim, S. Kang and J. Kim, *J. Electrochem. Soc.*, **158**, A275 (2011).
4. J. Kim and J. Cho, *Electrochem. Solid State Lett.*, **10**, A81 (2007).
5. J. Huang and Z. Jiang, *Electrochem. Solid State Lett.*, **11**, A116 (2008).
6. Y. Li, G.L. Pan, J.W. Liu and X.P. Gao, *J. Electrochem. Soc.*, **156**, A495 (2009).
7. J. Kim, S. Kim, H. Gwon, W. Yoon and K. Kang, *Electrochim. Acta*, **54**, 5914 (2009).
8. D. Wang, H. Xu, M. Gu and C. Chen, *Electrochem. Commun.*, **11**, 50 (2009).
9. S. Huang, Z. Wen, X. Zhu and X. Yang, *J. Electrochem. Soc.*, **152**, A1301 (2005).
10. B. Tian, H. Xiang, L. Zhang, Z. Li and H. Wang, *Electrochim. Acta*, **55**, 5453 (2010).
11. J. Wolfenstine and J. L. Allen, *J. Power Sources*, **180**, 582 (2008).
12. T. Yia, J. Shu, Y. Zhu, X. Zhu, R. Zhu and A. Zhou, *J. Power Sources*, **195**, 285 (2010).
13. H. Zhao, Y. Li, Z. Zhu, J. Lin, Z. Tian and R.Wang, *Electrochim. Acta*, **53**, 7079 (2008).
14. C.H. Chen, J.T. Vaughey, A.N. Jansen, D.W. Dees, A.J. Kahaian, T. Goacher and M.M. Thackeray, *J. Electrochem. Soc.*, **148**, A102-A104 (2001).
17. B. Zhang, H. Du, B. Li and F. Kang, *Electrochem. Solid State Lett.*, **13**, A36 (2010).
18. G. Zhu, C. Wang and Y. Xia, *J. Electrochem. Soc.*, **158**, A102 (2011).
19. J. Gao, J. Ying, C. Jiang and C. Wan, *J. Power Sources,* **166**, 255 (2007).
20. H. Jung, J. Kim, B. Scrosati and Y. Sun, *J. Power Sources,* **196**, 7763 (2011).
21. J. H. Ryu, J. W. Kim, Y. Sung and S. M. Oh, *Electrochem. Solid State Lett.*, **7**, A306 (2004).
22. N. Takami, K. Hoshina and H. Inagaki, *J. Electrochem. Soc.*, **158**, A725 (2011).